Local determination of weak anisotropy parameters from qP-wave slowness and particle motion measurements [1] [2]

Xuyao Zheng[*)] and **Ivan Pšenčík**[*)]

[*)] *Geophysical Institute, Acad.Sci.of Czech Republic, Boční II, Praha 4, Czech Republic,*
e-mail: zheng@ig.cas.cz, ip@ig.cas.cz

Abstract

We propose an algorithm for local evaluation of weak anisotropy (WA) parameters from measurements of slowness vector components and/or of particle motions of qP waves at individual receivers in a borehole in a multi-azimuthal multiple-source offset VSP experiment. As a byproduct the algorithm yields approximate angular variation of qP-wave phase velocity. The formulae are derived under assumption of weak but arbitrary anisotropy and lateral inhomogeneity of the medium. The algorithm is thus independent of structural complexities between the source and the receiver. If complete slowness vector is determinable from observed data, then the information about polarization can be used as an independent additional constraint. If only the component of the slowness along the borehole can be determined from observations (which is mostly the case), the inversion without information about polarization is impossible. We present several systems of equations, which can be used when different numbers of components of the slowness vector are available. The SVD algorithm is used to solve an overdetermined system of linear equations for WA parameters for two test examples of synthetic multi-azimuthal multiple-source offset VSP data. The system of equations results from approximate first-order perturbation equations for the slowness and polarization vectors of the qP wave. Analysis of singular values and of variances of WA parameters is used for the estimation of chances to recover the sought parameters. Effects of varying number of profiles with sources and of noise added to "observed" data are illustrated. An important observation is that although, due to insuficient data, we often cannot recover all individual WA parameters with sufficient accuracy, angular phase velocity variation can be recovered rather well.

Key words: Weak anisotropy, weak anisotropy parameters, qP waves, slowness vector, polarization vector, local inversion, multi-azimuthal VSP

[1] Seismic Waves in Complex 3-D Structures, Report 11 (Department of Geophysics, Charles University, Prague 2001), pp.15-42

[2] accepted in PAGEOPH

INTRODUCTION

Let us consider a multi-azimuthal multiple-source offset VSP experiment with three-component downhole recordings not affected by a free surface. Attempts to determine anisotropy parameters from data measured in such an experiment are not new. In the first attempts, VTI anisotropy (transverse isotropy with vertical axis of symmetry) was considered and measured components of the slowness vector were used. The vertical component of the slowness vector was determined from the travel times recorded in a vertical borehole. For the determination of the horizontal component, White et al. (1983) used qP- and qS-wave travel times from two neighbouring boreholes. For the data recorded in a single borehole, Gaiser (1990) proposed an approach, in which he assumed lateral homogeneity of the overburden. This assumption allowed him to make use of the travel time reciprocity and to determine the horizontal components of the qP-wave slowness vector from travel times between sources and a given receiver. De Parscau (1991), Hsu et al. (1991) and recently Williamson et al. (2000) also assumed a VTI medium and generalized Gaiser's approach in several respects. They used polarization data as an additional source of information on the anisotropy. In addition to data related to qP waves, de Parscau (1991) and Hsu et al. (1991) also used the qSV-wave data. De Parscau removed Gaiser's assumption of lateral homogeneity of the overburden. Pšenčík and Zheng (1998) generalized Gaiser's approach for qP waves in anisotropic media of arbitrary symmetry assuming that the anisotropy is weak and the linearized formulae can be used. As shown by Mensch and Rasolofosaon (1997) or Pšenčík and Gajewski (1998), the linearized formulae yield sufficiently accurate results for upto 20% strong anisotropy. As de Parscau (1991), Pšenčík and Zheng (1998) also used polarization as an independent source of information about the local WA parameters distribution. As Gaiser (1990), they assumed that the medium was laterally homogeneous. Horne et al. (1998) used qP-wave slowness vector components and polarization information to reveal parameters of arbitrarily strong TI medium. Their method had potential to be applied even to media of lower symmetry than TI. To solve a non-linear problem resulting from the use of exact formulae, they used search strategy based on simulated annealing. Horne and Leaney (2000) extended a procedure similar to the above one to include qS waves and reflected waves. For qP waves, their procedure can be used for arbitrary anisotropy. In both cases, the authors successfully applied their approach to real data. Williamson et al. (2000) used an approach similar to Horne et al. (1998) and applied it to real data from a 3D VSP experiment performed over an assumingly VTI medium.

The formulae given in this paper represent a generalization of the above approaches for anisotropic media of arbitrary symmetry assuming that their anisotropy is weak. For higher symmetries, they represent their alternatives. Thanks to the assumption of weak anisotropy (WA), which is common for many real materials (Thomsen, 1986), the formulae have a simple explicit and transparent form and broad applicability. They can be used for the local determination of upto 15 qP-wave WA parameters (generalization of Thomsen's (1986) parameters) in close vicinity of receivers situated in a borehole. The medium between source and receiver can be arbitrarily complex. As the input data we use qP-wave slownesses and polarizations. Our approach is as follows. For each receiver we find a reference isotropic medium, from which the sought weakly anisotropic medium differs only slightly. Then we can express the qP-wave slowness and the polarization vector in the weakly anisotropic medium using the formulae relating them linearly to the WA parameters specifying anisotropy of the medium (Pšenčík and Gajewski, 1998). For the estimation of components of the slowness vector and polarization, the parametric wavefield decomposition proposed by Esmersoy (1990) and extended by Leaney (1990) can be used. In this and related techniques, often only a component of the slowness vector along the borehole can be determined from observations. In such a case, the use of the polarization information becomes inevitable. With the information about slowness and polarization available, an overdetermined system of linear equations at each receiver can be constructed, from which the WA parameters can be determined.

In the next two sections, we derive basic equations for qP waves. In further sections, we illustrate the use of these equations to invert data from two synthetic experiments, see Figure 1. The SVD (singular value decomposition) algorithm is used for solving the system of linear equations in both cases. We call the first model VTI and the second TI. In the first, the studied medium is assumed to be laterally homogeneous, of VTI symmetry. In the second experiment, synthetic multi-azimuthal multiple-source offset VSP experiment is carried out over a laterally inhomogeneous TI medium with tilted axis of symmetry. Since the axis of symmetry is non-vertical and unknown, all 15 qP-wave WA parameters are sought in the process of inversion in the TI model. The "observed" seismograms were generated by the ANRAY package (Gajewski and Pšenčík, 1990). Analysis of singular values and variances of WA parameters is used to estimate chances to recover individual sought parameters. Effects of the ray coverage and of noise in data are briefly described.

PERTURBATION FORMULAE

Let us consider a Cartesian coordinate system (x, y, z), with positive z-axis pointing down along the borehole, see Figure 1. Furthermore, in the vicinity of a receiver let us define a reference isotropic medium, from which the sought local WA medium differs only slightly. The reference medium is specified by the P and S wave velocities α and β, which can differ from receiver to receiver. In the reference isotropic medium, we introduce three mutually perpendicular unit vectors (in the component notation) $e_i^{(1)}$, $e_i^{(2)}$ and $e_i^{(3)}$ so that the vector $e_i^{(3)}$ is parallel to the polarization vector of the P wave in the reference isotropic medium. The vector $e_i^{(3)}$ is also parallel to the P-wave phase normal n_i since in an isotropic medium the phase normal and polarization vector of a P wave are identical, i.e., $e_i^{(3)} = n_i$. The vectors $e_i^{(1)}$ and $e_i^{(2)}$ can be chosen arbitrarily in the plane perpendicular to n_i. A practical choice of vectors $e_i^{(1)}$, $e_i^{(2)}$ expressed in terms of components of the vector $e_i^{(3)}$ seems to be the following one, see Pšenčík and Gajewski (1998):

$$\vec{e}^{(1)} = D^{-1}(n_1 n_3, n_2 n_3, n_3^2 - 1), \quad \vec{e}^{(2)} = D^{-1}(-n_2, n_1, 0), \quad \vec{e}^{(3)} = \vec{n} = (n_1, n_2, n_3), \tag{1}$$

where

$$D = (n_1^2 + n_2^2)^{1/2}, \quad n_1^2 + n_2^2 + n_3^2 = 1. \tag{2}$$

Let us specify the phase normal as

$$\vec{n} = (\cos\varphi \sin\theta, \sin\varphi \sin\theta, \cos\theta). \tag{3}$$

Here φ denotes an azimuthal angle, θ a polar angle, ($0 \leq \varphi \leq 2\pi$, $0 \leq \theta \leq \pi$). In this case we have $D = \sin\theta$ and vectors $\vec{e}^{(1)}$ and $\vec{e}^{(2)}$ from Eq.(1) can be rewritten in the form

$$\vec{e}^{(1)} = (\cos\varphi\cos\theta, \sin\varphi\cos\theta, -\sin\theta), \quad \vec{e}^{(2)} = (-\sin\varphi, \cos\varphi, 0). \tag{4}$$

For the sake of simplicity, we use the specification (1) in terms of the components of the phase normal in the following.

First, we present perturbation formulae for the qP-wave polarization vector, then for the slowness vector.

Perturbation formula for polarization

The deviation Δg_i of the polarization vector of a qP wave in an anisotropic medium from the orientation of the polarization vector of the corresponding P wave in a reference isotropic medium, specified by the P- and S-wave velocities α and β, is given by the formula, see Pšenčík (1998)

$$\Delta g_i = \alpha \frac{\partial \Delta\tau}{\partial q_I} e_i^{(I)} + \frac{B_{13} e_i^{(1)}}{\alpha^2 - \beta^2} + \frac{B_{23} e_i^{(2)}}{\alpha^2 - \beta^2}. \tag{5}$$

The symbols B_{mn} denote elements of the *weak anisotropy* matrix,

$$B_{mn} = \Delta a_{ijkl} e_i^{(m)} e_j^{(3)} e_l^{(3)} e_k^{(n)}. \tag{6}$$

The symbol Δa_{ijkl} in (6) denotes the deviation of elastic parameters of the anisotropic medium from elastic parameters defining the isotropic reference medium. Explicit expressions for B_{13} and B_{23} for a general case and for the case of a VTI medium are given in the Appendix. The symbols q_I ($I = 1, 2$) in (5) denote local Cartesian coordinates (the ray-centered coordinates, see Pšenčík, 1998) in the plane perpendicular to the phase normal n_i. The coordinate q_I is specified by the vector $\vec{e}^{(I)}$. The symbol $\Delta\tau$ in (5) denotes a difference between the travel times in the anisotropic and reference isotropic media.

The first term on the RHS of Eq.(5) represents a correction of the slowness vector at a receiver from its orientation in the reference isotropic medium. This correction is due to the perturbation of the phase front, which, in turn, is due to the perturbation Δa_{ijkl}. This term can be determined by integration along the ray in the reference isotropic medium, see, e.g., Farra & Le Bégat (1995). Here, we evaluate this term from the observed data.

The second and third terms on the RHS of Eq.(5) represent deviations of the polarization vector of the qP wave from its slowness vector. They can also be obtained by the use of the perturbation method, see Jech & Pšenčík (1989), Pšenčík & Gajewski (1998).

All terms in (5) lead to the deviation of the polarization vector from the direction $e_i^{(3)} = n_i$ of the polarization vector in the reference isotropic medium. The terms in Eq.(5) remain non-zero even in homogeneous media.

Using (5), we can write the first-order expression for the polarization vector in an arbitrary WA medium in the following form

$$g_i \sim n_i + \Delta g_i = n_i + \alpha \frac{\partial \Delta\tau}{\partial q_I} e_i^{(I)} + \frac{B_{13} e_i^{(1)}}{\alpha^2 - \beta^2} + \frac{B_{23} e_i^{(2)}}{\alpha^2 - \beta^2}. \tag{7}$$

Multiplying Eq.(7) by $e_i^{(K)}$, $K = 1, 2$, we get the following two approximate equations

$$\alpha \frac{\partial \Delta\tau}{\partial q_K} + \frac{B_{K3}}{\alpha^2 - \beta^2} = g_i e_i^{(K)}. \tag{8}$$

The RHS of Eqs.(8) can be determined from observations. The second term on the LHS of Eqs.(8) is related to the sought WA parameters through the term B_{K3}, see Eqs.(A1b) and (A1c). The partial derivative in the first term on the LHS of Eqs.(8) can be rewritten as follows:

$$\frac{\partial \Delta\tau}{\partial q_K} = p_i e_i^{(K)} - p_i^0 e_i^{(K)} = p_i e_i^{(K)}. \tag{9}$$

Here p_i is the slowness vector of the qP wave in the anisotropic medium, p_i^0 is the slowness vector of the corresponding P wave in the reference isotropic medium. The vector p_i^0 is parallel to n_i and thus perpendicular to $e_i^{(K)}$. Eqs.(8) can be now rewritten into the following form

$$\alpha p_i e_i^{(K)} + \frac{B_{K3}}{\alpha^2 - \beta^2} = g_i e_i^{(K)}. \tag{10}$$

The slowness vector at a receiver can be expressed in the following way:

$$p_i = p_i^0 + \Delta\xi i_i + \Delta\zeta j_i + \Delta\eta k_i = (\xi + \Delta\xi) i_i + (\zeta + \Delta\zeta) j_i + (\eta + \Delta\eta) k_i. \tag{11}$$

The symbols i_i, j_i and k_i represent i-th components of unit vectors along the $x-$, $y-$ and $z-$axis, respectively. The symbols ξ, ζ and η denote sizes of projections of the slowness vector p_i^0 onto vectors i_i, j_i and k_i. The slowness vector p_i^0 reads

$$p_i^0 = \alpha^{-1} n_i. \tag{12}$$

This means that ξ, ζ and η in Eq.(11) are

$$\xi = \frac{n_1}{\alpha}, \quad \zeta = \frac{n_2}{\alpha}, \quad \eta = \frac{n_3}{\alpha}. \tag{13}$$

Inserting Eq.(11) into Eqs.(10), we get the following set of two equations

$$\frac{B_{K3}}{\alpha^2 - \beta^2} + \alpha\Delta\xi e_1^{(K)} + \alpha\Delta\zeta e_2^{(K)} + \alpha\Delta\eta e_3^{(K)} = g_i e_i^{(K)}. \tag{14}$$

Eqs.(14) are equations for 15 WA parameters and three quantities specifying deviation of p_i from $p_i^{(0)}$.

Perturbation formula for slowness

We can express the square of the qP-wave slowness c^{-2} in a WA medium using the following approximate formula (see, e.g., Pšenčík and Gajewski, 1998)

$$c^{-2} = \alpha^{-2}(1 - \frac{B_{33}}{\alpha^2}). \tag{15}$$

Neglecting second-order terms of $\Delta\xi$, $\Delta\zeta$ and $\Delta\eta$, Eq.(11) yields

$$c^{-2} = p_i p_i = \alpha^{-2}(1 + 2\alpha^2\xi\Delta\xi + 2\alpha^2\zeta\Delta\zeta + 2\alpha^2\eta\Delta\eta). \tag{16}$$

Comparison of the RHS of Eqs.(15) and (16) yields the following formula

$$B_{33} + 2\alpha^4\xi\Delta\xi + 2\alpha^4\zeta\Delta\zeta + 2\alpha^4\eta\Delta\eta = 0. \tag{17}$$

Expressions for B_{33} for general anisotropy and for a VTI medium can be found in the Appendix, Eqs.(A1a) and (A3a).

EQUATIONS FOR INVERSION - GENERAL WEAK ANISOTROPY

Eqs. (14) and (17) represent a set of equations for the WA parameters and for perturbations $\Delta\xi$, $\Delta\zeta$ and $\Delta\eta$ of the slowness vector, for each source-receiver pair. In most applications, we can assume the quantity $\Delta\eta$ to be known since $(\eta + \Delta\eta)k_i$ is, approximately, the z-component of the slowness vector p_i, which can be determined from travel time measurements in a borehole.

Let us first consider the case, in which all the components of the slowness vector are determinable from observations, i.e., in addition to $\Delta\eta$, also the deviations $\Delta\xi$ and $\Delta\zeta$ can be considered to be known. The slowness vector components could be determined, for example, from measurements in nearby wells, see White et al. (1983), under assumption of lateral homogeneity of the medium (Gaiser, 1990) or under another assumption controlling behaviour of the slowness vector. Knowledge of all the three components implies knowledge of the square of the slowness c^{-2}, see Eq.(16). In such a case, Eqs.(14) and (17) (or (15)) can be rewritten into the form

$$B_{K3} = (\alpha^2 - \beta^2)\Big(g_i e_i^{(K)} - \alpha\Delta\xi e_1^{(K)} - \alpha\Delta\zeta e_2^{(K)} - \alpha\Delta\eta e_3^{(K)}\Big), \tag{18}$$

$$B_{33} = \alpha^2(1 - \alpha^2 c^{-2}). \tag{19}$$

For N_S sources generating considered waves recorded at a given receiver, Eqs.(18) and (19) represent a set of 3 N_S linear equations for 15 WA parameters (A2). The WA parameters enter Eqs.(18) and (19) through the elements of the WA matrix B_{mn} given in Eqs.(A1). In this special formulation, we can consider equations for the slowness separately from equations for the polarization. Use of all equations together allows reduction of the number of sources N_S.

Let us now consider the case, in which, in addition to $\Delta\eta$, only the deviation $\Delta\zeta$ can be determined from observations, the perturbation $\Delta\xi$ being unknown. Then, instead of solving a large set of 3 N_S equations for 15 WA parameters and N_S values of $\Delta\xi$, it is more efficient to eliminate $\Delta\xi$ from Eqs.(14) and (17). In such a way, we arrive to the following two equations

$$(\alpha^2-\beta^2)^{-1}\xi B_{K3} - \frac{1}{2}\alpha^{-3}B_{33}e_1^{(K)} = \xi g_i e_i^{(K)} - \alpha X^{(K)}\Delta\zeta - \alpha\Delta\eta(\xi e_3^{(K)} - \eta e_1^{(K)}), \tag{20}$$

where

$$X^{(K)} = \xi e_2^{(K)} - \zeta e_1^{(K)}. \tag{21}$$

For N_S sources, we thus have 2 N_S equations for 15 WA parameters (A2) at each receiver. In this formulation, it is not possible to deal with information about the slowness vector and polarization separately. Without the information about polarization the inversion is impossible.

If none of the deviations $\Delta\xi$ and $\Delta\zeta$ is known, which is the case in laterally inhomogeneous media, we can eliminate $\Delta\zeta$ from Eqs.(20) and get a single equation

$$(\alpha^2-\beta^2)^{-1}(B_{13}X^{(2)} - B_{23}X^{(1)}) - \frac{1}{2}\alpha^{-2}B_{33}\eta =$$

$$(X^{(2)}e_i^{(1)} - X^{(1)}e_i^{(2)})g_i + \alpha\Delta\eta(X^{(1)}e_3^{(2)} - X^{(2)}e_3^{(1)} + \alpha\eta^2). \tag{22}$$

For N_S sources, we have a system of N_S equations for 15 WA parameters. If a higher anisotropy symmetry is not assumed, N_S must be larger than 15. Information on the slowness vector and polarization must be used together.

SYNTHETIC EXAMPLES

Model and configuration of the experiment

For the following tests we use the VSP configuration shown schematically in Figure 1. The whole model is confined in a model box whose horizontal dimensions are 10 × 10 km. The borehole is situated in the center of the model. We consider two types of models. First, we test the above described approach on a simple model of a vertically inhomogeneous VTI medium. Such a type of anisotropic symmetry has been studied by, for example, White et al. (1983), Gaiser (1990), de Parscau (1991), Williamson et al. (2000). Then we test the approach on a model of a laterally inhomogeneous TI medium with an inclined axis of symmetry. We call the above models VTI and TI, respectively. For simplicity, the same density-normalized elastic parameters are used at the top and the bottom surfaces of the VTI and TI model. Anisotropy of the models is about 8%. At the top surface of each model, the density-normalized elastic parameters A_{ij}, in (km/s)^2, are: $A_{11}=A_{22}=15.71$, $A_{33}=13.39$, $A_{12}=5.05$, $A_{13}=A_{23}=4.46$, $A_{44}=A_{55}=4.98$, $A_{66}=\frac{1}{2}(A_{11}-A_{12})=5.33$. At each bottom surface: $A_{11}=35.348$, $A_{33}=30.128$, $A_{12}=11.363$, $A_{13}=10.035$, $A_{44}=11.205$. In the VTI model, the top and the bottom surfaces are the horizontal surfaces at depths of 0 and 5 km. In the TI model, the axis of symmetry at the horizontal top surface at the depth of 0 km is rotated by 80^o from the z-axis in the (x,z)-plane, and then by 25^o around the z-axis. The axis of symmetry at the bottom surface is rotated by 90^o from the $z-$axis in the (x, z)-plane (thus, the symmetry of the medium at the bottom surface is HTI). The bottom surface is an inclined plane intersecting the vertical border of the model $x = -5$ km at the depth of 9 km and the border $x = 5$ at the depth of 1 km. Between the top and the bottom surfaces the elastic parameters are determined by linear interpolation. Since both surfaces are horizontal in the case of the VTI model, the variation of elastic parameters with depth is the same everywhere and the model is laterally homogeneous. The inclined bottom surface of the TI model introduces lateral inhomogeneity into the model. Also note that while anisotropy in the VTI model is the same throughout the model (only its strength is varying with depth), anisotropy of the TI model varies with depth.

Due to the axial symmetry of the VTI model, a single, arbitrarily oriented, surface profile with sources to one side of the borehole is sufficient. In the TI model, we consider 3 or 5 surface profiles with their center at the mouth of the borehole, see Figure 1. The 3 profiles are distributed uniformly with the step in the angle between them equal 60^o. It means that the 3 profiles can be associated successively with 0^o, 60^o and 120^o, measured from the positive x- axis. The 5 profiles are associated with angles 0^o, 30^o, 60^o, 120^o and 150^o.

Each profile contains 9 sources at each side of the borehole, starting at 0.1 km from the mouth of the borehole and separated by 0.1 km. The vertical borehole contains 13 three-component receivers starting at a depth of 0.1 km and separated by 0.05 km, see Figure 1. The free surface effects are neglected throughout the experiment. From the above configuration, we can see that observations along the single profile in the VTI model yield 18 independent equations (see Eqs.(A3) and Eqs.(18) and (19)) for 3 WA parameters at each receiver. In the TI model, the system of 3 profiles yields 54 equations (see Eq.(22)) for 15 WA parameters at each receiver. The system of 5 profiles yields 90 equations for 15 WA parameters. Let us note that independently of the number of sources used along the 3 profiles, we cannot, in principle, recover all the 15 WA parameters. Some of the WA parameters can be recovered only in a linear combination with others, see the discussion after Eq.(17) of Pšenčík and Gajewski (1998). The case of the 5 profiles represents, according to the mentioned authors, the minimum of profiles allowing, theoretically, a complete recovery of all 15 WA parameters.

Data

For both models, synthetic seismograms were generated using the program package ANRAY (Gajewski and Pšenčík, 1990). From the seismograms, arrival times were picked and particle motion diagrams were constructed. Picked travel times from five neighbouring receivers were used to determine the best fitting hyperbola, from which the partial derivative of the travel time with respect to the $z-$coordinate (coordinate along the borehole) was found. In this way $\Delta\eta$ used in (18), (19), (20) and (22) could be determined. The above described way of the determination of the components of the slowness vector along the borehole causes inacuracies in its determination at shallowest and deepest receivers, see further. To find the polarization vector g_i, a straight line best fitting (in the least square sense) the observed particle motion was sought. Alternatively, the parametric inversion method of Esmersoy (1990), extended by Leaney (1990), could be used to recover $\Delta\eta$ and the vertical component of the polarization vector g_i.

The observed travel times were used to determine an approximate 1-D distribution of the P-wave velocity α. The S-wave velocity β was taken as $\beta = \alpha/\sqrt{3}$. In this way, the reference isotropic model was built. Then the rays from the source to individual receivers were traced in the reference medium. Normalized slowness vectors at receivers yielded the phase normal n_i, see Eq.(3), with respect to which, the vectors $e_i^{(1)}$ and $e_i^{(2)}$ were defined.

For solving the resulting system of equations, the SVD method was used. The singular values and variances were used to estimate chances to recover individual WA parameters. The variance $\sigma(\epsilon_i)$ of a WA parameter ϵ_i was calculated from the singular values λ_i (i=1,...,15) and the 15 $\times$ 15 orthogonal matrix V_{ij} that spans the model space of the WA parameters ($V_{ji}V_{jk} = I_{ik}$, I_{ik} being the 15 $\times$ 15 identity matrix):

$$\sigma^2(\epsilon_i) = \sigma_0^2 \sum_{j=1}^{15} (V_{ji}/\lambda_j)^2. \tag{23}$$

The symbol σ_0^2 denotes a variance of a polarization vector or of a vertical component of a slowness vector. Both variances are assumed to be the same and equal one in the following. The variances depend on the number of the used profiles, on the illumination of receivers and also on the chosen reference velocity. For analysis of the data, we used the relative singular values. At each receiver they were calculated as ratios of the given singular value and the maximum one.

In the following, we present results of inversion for the above-mentioned two experiments.

VTI model

Eqs.(18) and (19) with the elements of the WA matrix B_{mn} specified for a VTI medium, see (A3), are used for this model. This means that the number of sought WA parameters reduces from 15 to only 3: ϵ_x, ϵ_z and δ_x. Because of the model symmetry, the slowness vector is confined to a vertical plane and has only two non-zero components. The vertical component is determined by numerical differentiation of travel times along the borehole. The horizontal component is determined with the use of reciprocity of travel times by a similar numerical differentiation along a surface profile of sources. Since the polarization formula (18) is sensitive to the choice of the reference medium, we use the reference velocity determined from the slowness vector. In other words, we use the velocity c determined from Eq.(15) as the reference velocity for inverting Eq.(18). Because a different reference isotropic medium is used at each receiver, we show inverted values of elastic parameters A_{11}, A_{33} and $A_{13} + 2A_{55}$ in Figure 2 instead of the above mentioned WA parameters.

Except for the "polarization" method, the relative singular values are relatively close to each other at each receiver, indicating small condition number. This means that chances to retrieve all the three WA parameters independently are high. The smallest relative singular values are of the order 10^{-1}. In the "polarization" method, one singular value is very small indicating interdependency of the 3 WA parameters. Nonetheless, even in this case, with the small singular value ignored, the inversion yields acceptable results, see below.

The three frames in Figure 2 show, from the left to the right, the results obtained with the "slowness" equation (19) (left), the results obtained with the "polarization" equation (18) (middle), and the results obtained from the use of both equations together (right). The solid lines represent the exact model, the symbols correspond to the specified inverted parameters. In the "slowness" frame, we can see relatively well inverted parameters A_{11} and A_{33}, the determination of $A_{13} + 2A_{55}$ not being so satisfactory. The "polarization" frame gives much better fit although, as mentioned above, one of the singular values had to be ignored. The best results are, however, obtained when both equations (18) and (19) are used together. The relative errors in the determination of the parameters A_{11}, A_{33} and $A_{13} + 2A_{55}$, for all the receivers except the shallowest and the deepest one, do not exceed 2%.

Remarkably large deviations from the exact values for the shallowest and deepest receivers are caused by inaccuracies in the determination of the slowness vector at the ends of the best fitting hyperbola, mentioned in the previous section. This also affects results obtained with the "polarization" equation (18) since Eq.(18) contains the slowness vector.

TI model

The results of this section are based on the use of Eq.(22). Now the observed data yield only the component of the slowness vector parallel to the borehole. Thus without information about the polarization the inversion cannot be performed.

Figure 3 shows the relative singular values of the problem as a function of depth. The upper plot shows the relative singular values for the case of 3 profiles, the lower plot for the case of 5 profiles. We can see that for 3 profiles, the span of the relative singular values is very large, i.e., the condition number is large. Three singular values are smaller or equal 10^{-6}. The next two singular values are between 10^{-3} and 10^{-2}. This indicates interdependency of some of the sought WA parameters. This is not a surprise because 3 profiles are insufficient for independent recovery of all 15 qP-wave WA parameters. The situation changes dramatically when two additional profiles are added (lower plot in Figure 3). The lowest relative singular values are now around 10^{-3}, mostly for the shallowest receivers. This means that chances for independent recovery of individual WA parameters are much larger using 5 profiles. From both plots in Figure 3 we can see that, except for shallow receivers, the distribution of singular values depends only slightly on receiver depth.

Figures 4a and 4b show variances of all 15 qP-wave WA parameters for the case of 3 and 5 profiles, respectively. The variances are calculated from the formula (23) with lower values indicating a higher probability of the determination of the corresponding parameter. In Figure 4a, we can clearly see which WA parameters are mainly responsible for the low values of singular values in the upper plot of Figure 3. We can see that there are 6 WA parameters, which have no chance to be resolved independently. They are: ϵ_y, δ_z, χ_x, ϵ_{16}, ϵ_{24} and ϵ_{26}. This observation is in agreement with conclusions of Pšenčík and Gajewski (1998) if we take into account that none of the 3 considered profiles is situated in the plane (y, z). All the above listed parameters are related to prevailingly horizontal propagation, and in a horizontal plane to the propagation along the y-axis, see Eqs.(A1). This is a consequence of insufficient horizontal illumination, especially of deeper receivers. Another consequence is the increase of variances with depth for most of the WA parameters. Extension of profiles or, better, increase of their number can reduce this problem, see Figure 4b. The variances dramatically change when two additional profiles are considered. The variances are now generally small and differences between them are substantially smaller. We can observe slightly larger variances for the parameters ϵ_x, ϵ_y, δ_x, δ_y, δ_z and χ_z. The addition of the two profiles improved illumination of deeper receivers so that only a few variances increase with depth. Let us note that Figure 4b would not change much if an additional profile were added.

Figure 5 shows the relative errors of the inverted parameters. Each figure shows 3 bar charts corresponding to the receiver 4 (top), 7 (middle) and 10 (bottom). The values of the exact WA parameters for these receivers are given in Table 1. Figure 5a shows the results of the inversion for the case of 3 profiles with all singular values, including the small ones in Figure 3a, considered. As we could expect from the analysis of singular values and variances, some relative errors reach values of 100% and more (all values larger than 100% are displayed as 100% in Figure 5). This concerns the 6 WA parameters with extremely high variances in Figure 4a. In addition to them, high relative errors can also be observed for the parameters δ_y, ϵ_{34}, χ_y and χ_z. This is again in agreement with observations of Pšenčík and Gajewski (1998) for the case of number of profiles less than 5, of which none is situated in the plane (y, z). The results of the inversion can be considerably improved if we ignore the lowest three singular values in the upper frame of Figure 3. This is shown in Figure 5b. Further substantial improvement can be reached if two additional profiles are considered, see Figure 5c. Even in this case, however, the above listed six WA parameters with high variances still have large relative errors. This could be fixed by extension of the profiles or by their different orientation, in other words by a better illumination of receivers. This is a task for future studies.

In Figure 6, equal area plots of isolines of the qP-wave phase velocity obtained from inversion (thin lines) and from the exact model (solid lines) are compared. The solid circles indicate positions of the axes of symmetry, which are identical with the longitudinal directions (directions, in which slowness and polarization vectors are parallel, Helbig, 1994), in the exact model. The open circles indicate longitudinal directions obtained from inversion. The left column shows results for 3 profiles, the right column for 5 profiles. In each column, results for the receivers 4, 7 and 10 situated at depths z=0.25, 0.4 and 0.55 km are shown. The results of inversion for 3 profiles would make no sense unless, at least three smallest singular values shown in the upper frame of Figure 3 were ignored. In Figure 5b we illustrated how removal of small singular values reduces relative errors. For this reason, we ignored all relative singular values substantially smaller than 10^{-2} in the following results. Actually it means that we ignored 4 singular values in the case of 3 profiles and 1 singular value in the case of 5 profiles.

We can see that the thin line curves in Figure 6 have more complicated form than the solid line curves, which correspond to the TI model. This means that the inverted phase velocity does not correspond any more to the TI symmetry. For this reason we compare the longitudinal directions instead of the axes of symmetry. As expected, the fit between exact and inverted phase velocities is better for 5 profiles. The best overall fit can be observed for the receiver 4. Isolines of the exact and inverted model fit each other well not only in the centre of the circle, i.e., for vertical direction, but also at the border of the circle, i.e., for horizontal direction. This picture changes when moving to deeper receivers. For the receiver 10, a good fit can be observed at the centre of the circle. Towards the border of the circle, misfit increases. This indicates insuffîcent illumination of receivers with increasing depth. While the angles of rays illuminating the receiver 4 vary from 23^0 to 79^0 (0^0 specifies vertical direction), the angles of rays illuminating the receiver 10 vary from 11^0 to 63^0. Thus the receiver 10 is insufficiently illuminated by nearly horizontally propagating rays. Longitudinal directions are obviously better determined for 5 profiles.

Figure 7 shows, in the same display and for the same specification as Figure 6, effects of the 10% random noise added separately to each component of the observed seismograms. The noise effects significantly angular variation of the phase velocity and also the position of the minimum velocity. The results for the receiver 10 are unacceptable for both 3 and 5 profiles. This is because of the insufficient illumination of the receiver mentioned in the discussion of Figure 6. At receivers 4 and 7, slightly better results, especially longitudinal directions, are found for 5 profiles.

CONCLUSIONS

We present an algorithm for the local determination of the 15 WA parameters specifying qP-wave propagation in laterally varying, weakly anisotropic media of arbitrary symmetry. We show that for the determination of the WA parameters from observations in a multi-azimuthal multiple-source offset VSP experiment performed in such a complex structure, knowledge of arrival times and particle motions is necessary. Only under certain simplifying conditions (e.g. lateral homogeneity, measurements in a symmetry plane) information from travel times and particle motions can be used separately.

Performed tests show, in agreement with previous theoretical conclusions, that the minimum number of profiles necessary for independent retrieval of all 15 qP-wave WA parameters is five. Synthetic tests, however, also show that even with three profiles some interesting characteristics of the medium can be retrieved, e.g., an estimate of the longitudinal direction. This is because the WA parameters which cannot be obtained independently do not have substantial influence on the determination of phase velocity. Even with 10% noise in data, it is possible to make approximate estimates of anisotropy. Further and more thorough tests of the effects of noise are necessary.

In presented tests, a moderate anisotropy of about 8% was considered. It is desirable to test the described procedure on models with stronger or weaker anisotropy. We also plan to study the effects of different acquisition geometry, deviated wells, lateral inhomogeneity. We have already started tests with real data.

In the present study, our only source of information was the direct qP wave. Extension to reflected qP waves is straightforward. Derivation of formulae necessary for the use of the qS-wave information is planned. The study of qS waves is complicated by their coupling in inhomogeneous weakly anisotropic media, see e.g. Pšenčík (1998). Even if the qS waves are separated, their slownesses are given by non-linear formulae for symmetries lower than TI, which further complicates the procedure.

ACKNOWLEDGEMENTS

The authors appreciate very much stimulating reviews of Steve Horne and Soazig le Bégat. Critical comments of M.Baan, P.Bakker, V.Farra and V.Vavryčuk are also appreciated. This work was supported by the consortium project "Seismic waves in complex 3-D structures (SW3D)" and by the Grant Agency of the Czech Republic under the contract No. 205/00/1350. XZ is greateful for the support of the National Natural Science Foundation of China, No.49774230. The final part of this work was done during the stay of IP at CPGG, Universidade Federal da Bahia, Salvador, Brazil.

REFERENCES

de Parscau,J. (1991), *P- and SV-wave transversely isotropic phase velocities analysis from VSP data*, Geophys. J. Int., *107*, 629-638.

Esmersoy,C. (1990), *Inversion of P and SV waves from multicomponent offset vertical seismic profiles*, Geophysics, *55*, 39-50.

Farra,V. and Le Bégat,S. (1995), *Sensitivity of qP-wave travel times and polarization vectors to heterogeneity, anisotropy and interfaces*, Geophys. J. Int., *121*, 371-384.

Gaiser,J.E. (1990), *Transversely isotropic phase velocity analysis from slowness estimates*, J. Geophys. Res., *95*, 11241-11254.

Gajewski,D. and Pšenčík,I. (1990), *Vertical seismic profile synthetics by dynamic ray tracing in laterally varying layered anisotropic structures*, J.Geophys.Res., *95*, 11301-11315.

Helbig,K., *Foundations of anisotropy for exploration seismics* (Pergamon, Oxford 1994).

Horne,S.A. and Leaney,S. (2000), *Polarization and slowness component inversion for TI anisotropy*, Geophysical Prospecting, *48*, 779-788.

Horne,S.A., McGarrity,J.P., Sayers,C.M., Smith,R.L. and Wijnands,F., *Fractured reservoir characterisation using multi-azimuthal walkaway VSPs*, In *Expanded Abstracts, 68th Ann. Internat. Mtg.*, (Soc.Expl.Geophys., Tulsa 1998) pp. 1640-1643.

Hsu,K., Schoenberg,M. and Walsh,J., *Anisotropy from polarization and moveout*, In *Expanded Abstracts, 61th Ann. Internat. Mtg.*, (Soc.Expl.Geophys., Tulsa 1991) pp. 1526-1529.

Jech,J. and Pšenčík,I. (1989), *First-order perturbation method for anisotropic media*, Geophys. J. Int., *99*, 369-376.

Leaney,W.S., *Parametric wavefield decomposition and applications*, In *Expanded Abstracts, 60th Ann. Internat. Mtg.*, (Soc.Expl.Geophys., Tulsa 1990) pp. 1097-1100.

Mensch,T. and Rasolofosaon,P. (1997), *Elastic wave velocities in anisotropic media of arbitrary symmetry - generalization of Thomsen's parameters ε, δ and γ*, Geophys. J. Int., *128*, 43-64.

Pšenčík,I. (1998), *Green's functions for inhomogeneous weakly anisotropic media*, Geophys. J. Int., *135*, 279-288.

Pšenčík,I. and Gajewski,D. (1998), *Polarization, phase velocity and NMO velocity of qP waves in arbitrary weakly anisotropic media*, Geophysics, *63*, 1754-1766.

Pšenčík,I. and Zheng,X., *Determination of weak anisotropy parameters from the qP-wave particle motion measurements*, In *Seismic Waves in Complex 3-D Structures*, Report 7, (Dept.of Geophysics, Charles University, Prague 1998) pp. 299-306 (available online at "http://seis.karlov.mff.cuni.cz/papers/r7ip3.htm).

Thomsen,L. (1986), *Weak elastic anisotropy*, Geophysics, *51*, 1954-1966.

White,J.E., Martineau-Nicoletis,L and Monash,C. (1983), *Measured anisotropy in Pierre shale.* Geophysical Prospecting *31*, 709-725.

Williamson,P., Maocec.E. and Boelle,J-L., *Local estimation of anisotropy parameters from well seismic polarisation data*, In *Expanded Abstracts, 70th Ann. Internat. Mtg.*, (Soc.Expl.Geophys., Tulsa 2000) pp. 2241-2244.

APPENDIX

The elements B_{33}, B_{13} and B_{23} of the weak anisotropy matrix for an anisotropic medium of arbitrary symmetry read, see Pšenčík and Gajewski (1998):

$$B_{33} = 2\alpha^2[\epsilon_z n_3^4 + 2n_3^3(\epsilon_{34}n_2 + \epsilon_{35}n_1) + n_3^2(\delta_x n_1^2 + \delta_y n_2^2 + 2\chi_z n_1 n_2)$$
$$+2n_3(\chi_x n_1^2 n_2 + \chi_y n_1 n_2^2 + \epsilon_{15}n_1^3 + \epsilon_{24}n_2^3) + \epsilon_x n_1^4 + \delta_z n_1^2 n_2^2$$
$$+\epsilon_y n_2^4 + 2\epsilon_{16}n_1^3 n_2 + 2\epsilon_{26}n_1 n_2^3], \qquad (A1a)$$

$$B_{13} = \alpha^2 D^{-1}\Big[2\epsilon_z n_3^5 + n_3^4(\epsilon_{34}n_2 + \epsilon_{35}n_1) + n_3^3(\delta_x n_1^2 + \delta_y n_2^2 + 2\chi_z n_1 n_2 - 2\epsilon_z)$$
$$+n_3^2[(4\chi_x - 3\epsilon_{34})n_1^2 n_2 + (4\chi_y - 3\epsilon_{35})n_1 n_2^2 + (4\epsilon_{15} - 3\epsilon_{35})n_1^3 + (4\epsilon_{24} - 3\epsilon_{34})n_2^3]$$
$$+n_3[(2\delta_z - \delta_x - \delta_y)n_1^2 n_2^2 + 2(2\epsilon_{16} - \chi_z)n_1^3 n_2 + 2(2\epsilon_{26} - \chi_z)n_1 n_2^3 + (2\epsilon_x - \delta_x)n_1^4 + (2\epsilon_y - \delta_y)n_2^4]$$
$$-\chi_x n_1^2 n_2 - \chi_y n_1 n_2^2 - \epsilon_{15}n_1^3 - \epsilon_{24}n_2^3\Big] \qquad (A1b)$$

and

$$B_{23} = \alpha^2 D^{-1}\Big[n_3^3(\epsilon_{34}n_1 - \epsilon_{35}n_2) + n_3^2[(\delta_y - \delta_x)n_1 n_2 + \chi_z n_1^2 - \chi_z n_2^2]$$
$$+n_3[(2\chi_y - 3\epsilon_{15})n_1^2 n_2 - (2\chi_x - 3\epsilon_{24})n_1 n_2^2 + \chi_x n_1^3 - \chi_y n_2^3]$$
$$+(\delta_z - 2\epsilon_x)n_1^3 n_2 + (2\epsilon_y - \delta_z)n_1 n_2^3 + 3(\epsilon_{26} - \epsilon_{16})n_1^2 n_2^2 + \epsilon_{16}n_1^4 - \epsilon_{26}n_2^4\Big]. \qquad (A1c)$$

The quantity D is defined in Eq.(2) and the WA parameters appearing in (7) are defined as follows

$$\epsilon_x = \frac{A_{11} - \alpha^2}{2\alpha^2}, \quad \epsilon_y = \frac{A_{22} - \alpha^2}{2\alpha^2}, \quad \epsilon_z = \frac{A_{33} - \alpha^2}{2\alpha^2},$$
$$\delta_x = \frac{A_{13} + 2A_{55} - \alpha^2}{\alpha^2}, \quad \delta_y = \frac{A_{23} + 2A_{44} - \alpha^2}{\alpha^2}, \quad \delta_z = \frac{A_{12} + 2A_{66} - \alpha^2}{\alpha^2},$$
$$\chi_x = \frac{A_{14} + 2A_{56}}{\alpha^2}, \quad \chi_y = \frac{A_{25} + 2A_{46}}{\alpha^2}, \quad \chi_z = \frac{A_{36} + 2A_{45}}{\alpha^2},$$
$$\epsilon_{15} = \frac{A_{15}}{\alpha^2}, \quad \epsilon_{16} = \frac{A_{16}}{\alpha^2}, \quad \epsilon_{24} = \frac{A_{24}}{\alpha^2}, \quad \epsilon_{26} = \frac{A_{26}}{\alpha^2}, \quad \epsilon_{34} = \frac{A_{34}}{\alpha^2}, \quad \epsilon_{35} = \frac{A_{35}}{\alpha^2}. \qquad (A2)$$

The formulae (A1) simplify if a higher symmetry anisotropic media are considered. For the VTI medium considered in our experiments, Eqs.(A1) reduce to

$$B_{33} = 2\alpha^2[\epsilon_z n_3^4 + \delta_x n_3^2(1 - n_3^2) + \epsilon_x(1 - n_3^2)^2], \qquad (A3a)$$

$$B_{13} = \alpha^2 n_3(1 - n_3^2)^{1/2}[(\delta_x - 2\epsilon_z)n_3^2 - (\delta_x - 2\epsilon_x)(1 - n_3^2)] \qquad (A3b)$$

and

$$B_{23} = 0. \qquad (A3c)$$

TABLE AND FIGURE CAPTIONS

Table 1: Exact values of the WA parameters at the receivers 4, 7 and 10 in the TI model.

Figure 1: Multi-azimuthal multiple-source offset VSP experiment configuration: 5 radial surface profiles (the 3 profiles from the 3-profile experiment by solid lines) with 9 shots to each side of the borehole, with 0.1 km separation; 13 three-component receivers in the borehole with 0.05 km separation.

Figure 2: VTI model: comparison of exact (solid lines) and inverted (symbols) density-normalized elastic parameters using slowness equation (19) (left), polarization equations (18) (middle) and both equations (right).

Figure 3: TI model: Singular values corresponding to 15 qP-wave WA parameters as a function of depth obtained for 3 profiles and 5 profiles.

Figure 4: TI model: Variances of 15 qP-wave WA parameters as a function of depth obtained from system of equations (22) for 3 profiles and 5 profiles. The lower the value of variance, the better the chance to determine the corresponding parameter.

Figure 5: TI model: Relative errors (%) of 15 qP-wave WA parameters for noise-free data from 3 profiles with all singular values, with 3 smallest singular values ignored and from 5 profiles with all singular values, for receivers 4, 7 and 10. Equation (22) used.

Figure 6: TI model: Equal area plots of phase velocity obtained from inversion (thin lines) and for the exact model (thick lines). The open and solid circles: longitudinal axes. Four and one smallest singular values ignored for 3 and 5 profiles, respectively.

Figure 7: TI model: 10% random noise added to the "observed" data. Equal area plots of phase velocity obtained from inversion (thin lines) and for the exact model (thick lines). The open and solid circles: longitudinal axes. Four and one smallest singular values ignored for 3 and 5 profiles, respectively.

WA	receiver 4	receiver 7	receiver 10
ϵ_x	-.04370	-.04455	-.04534
ϵ_y	.00742	.00823	.00899
ϵ_z	.01813	.01825	.01836
δ_x	-.03027	-.03125	-.03216
δ_y	.02555	.02648	.02735
δ_z	-.03594	-.03655	-.03712
χ_x	-.00286	-.00268	-.00250
χ_y	-.01060	-.00992	-.00928
χ_z	-.02787	-.02607	-.02439
ϵ_{15}	-.00994	-.00930	-.00870
ϵ_{16}	-.02383	-.02229	-.02085
ϵ_{24}	-.00533	-.00499	-.00466
ϵ_{26}	-.02740	-.02563	-.02397
ϵ_{34}	-.00549	-.00513	-.00480
ϵ_{35}	-.01177	-.01101	-.01030

Table 1

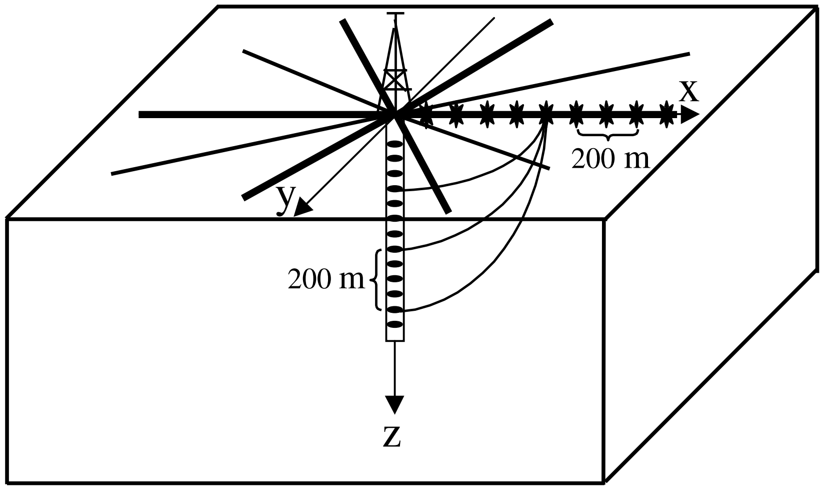

Figure 1

VTI INVERSION RESULTS

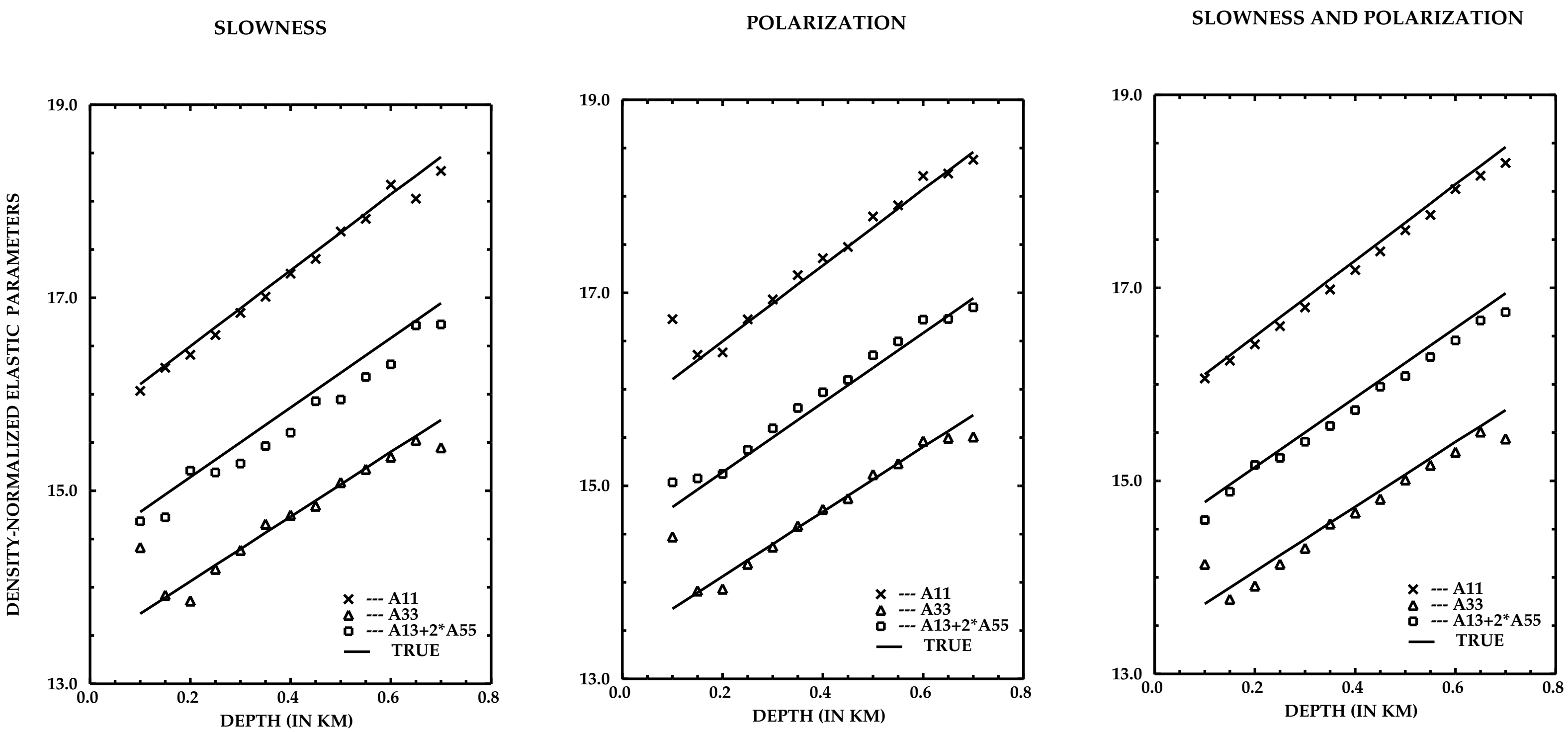

Figure 2

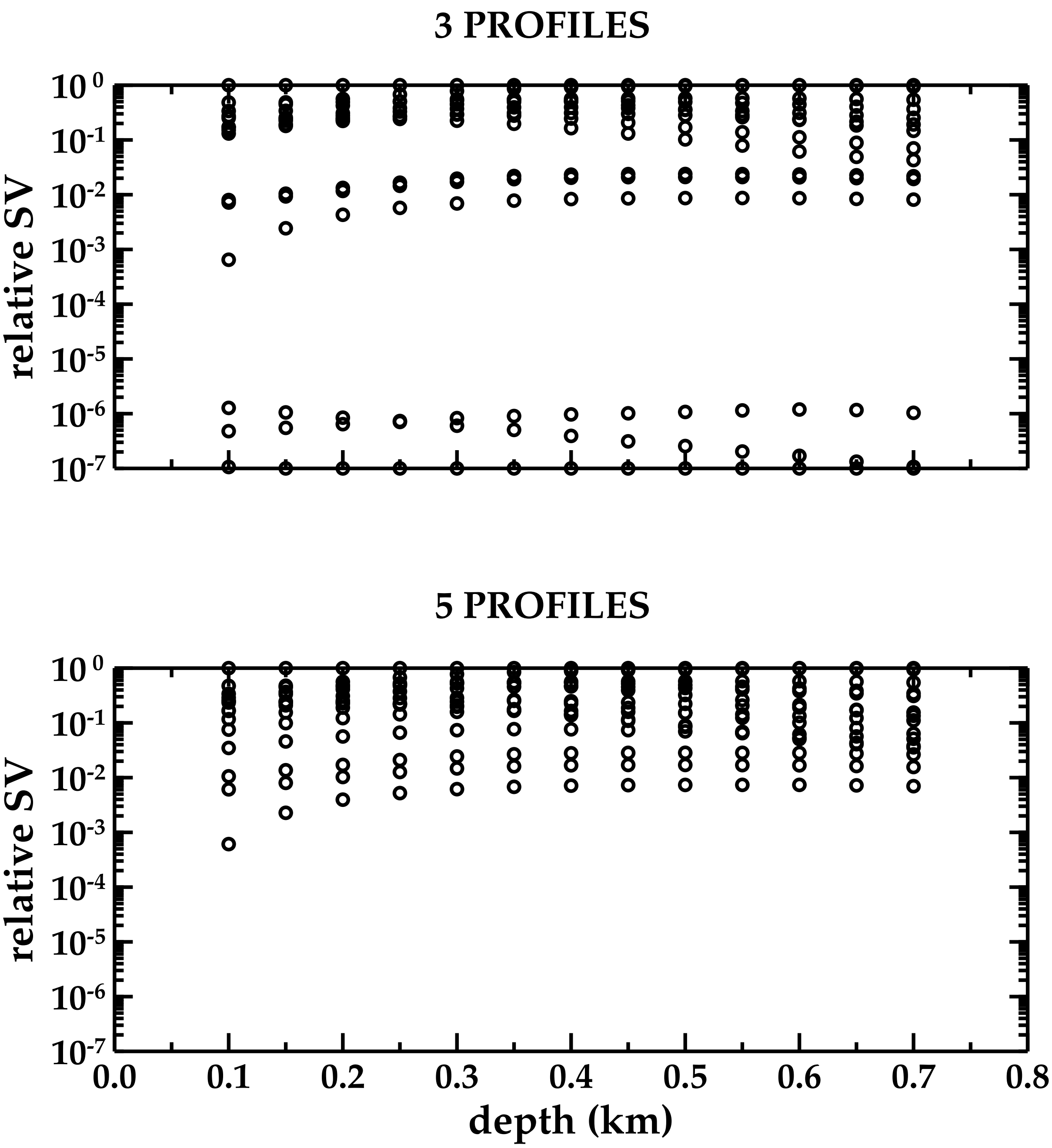
3 PROFILES
relative SV
10^0
10^{-1}
10^{-2}
10^{-3}
10^{-4}
10^{-5}
10^{-6}
10^{-7}
5 PROFILES
relative SV
10^0
10^{-1}
10^{-2}
10^{-3}
10^{-4}
10^{-5}
10^{-6}
10^{-7}
0.0
0.1
0.2
0.3
0.4
0.5
0.6
0.7
0.8
depth (km)

Figure 3

3 PROFILES

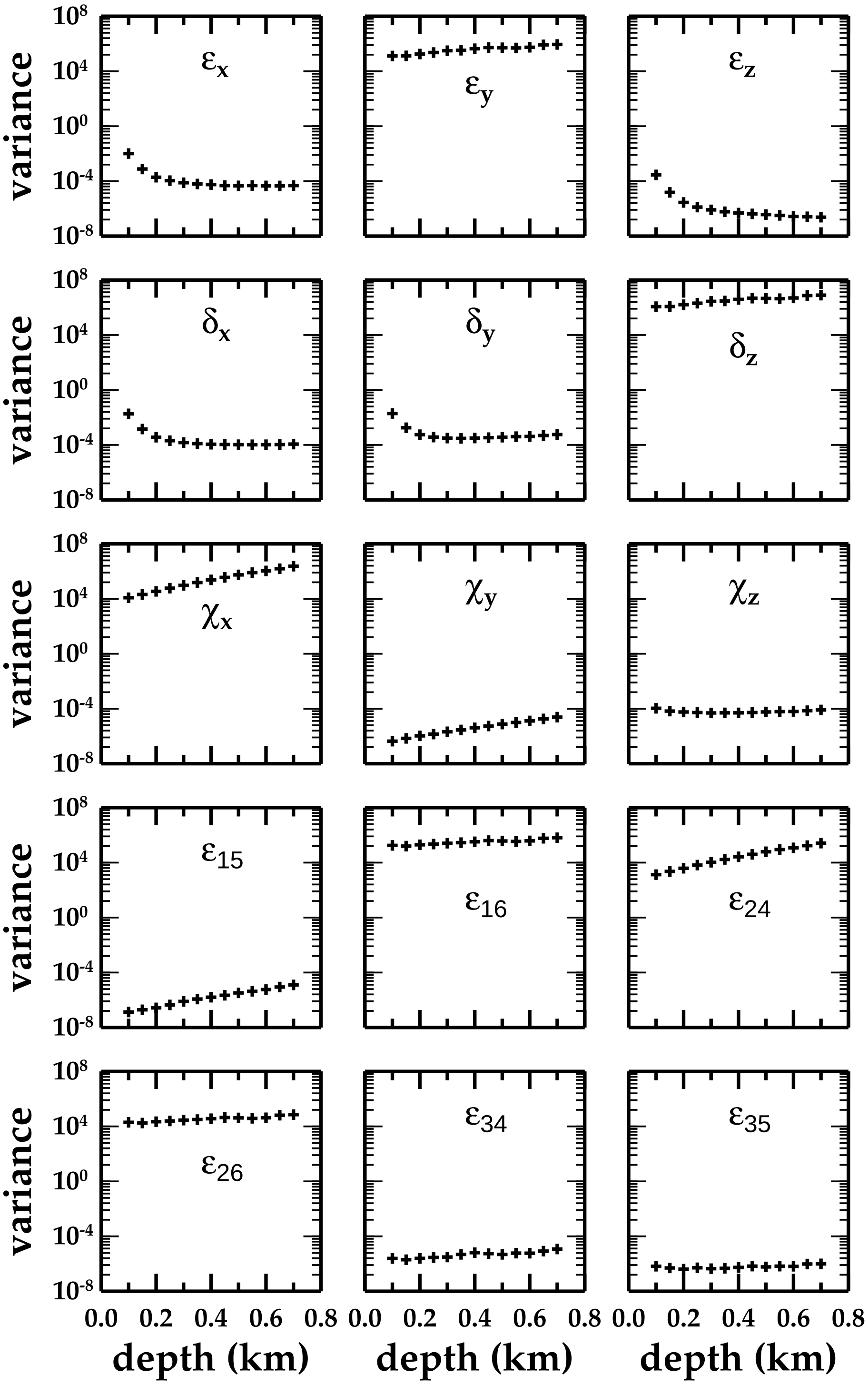

Figure 4a

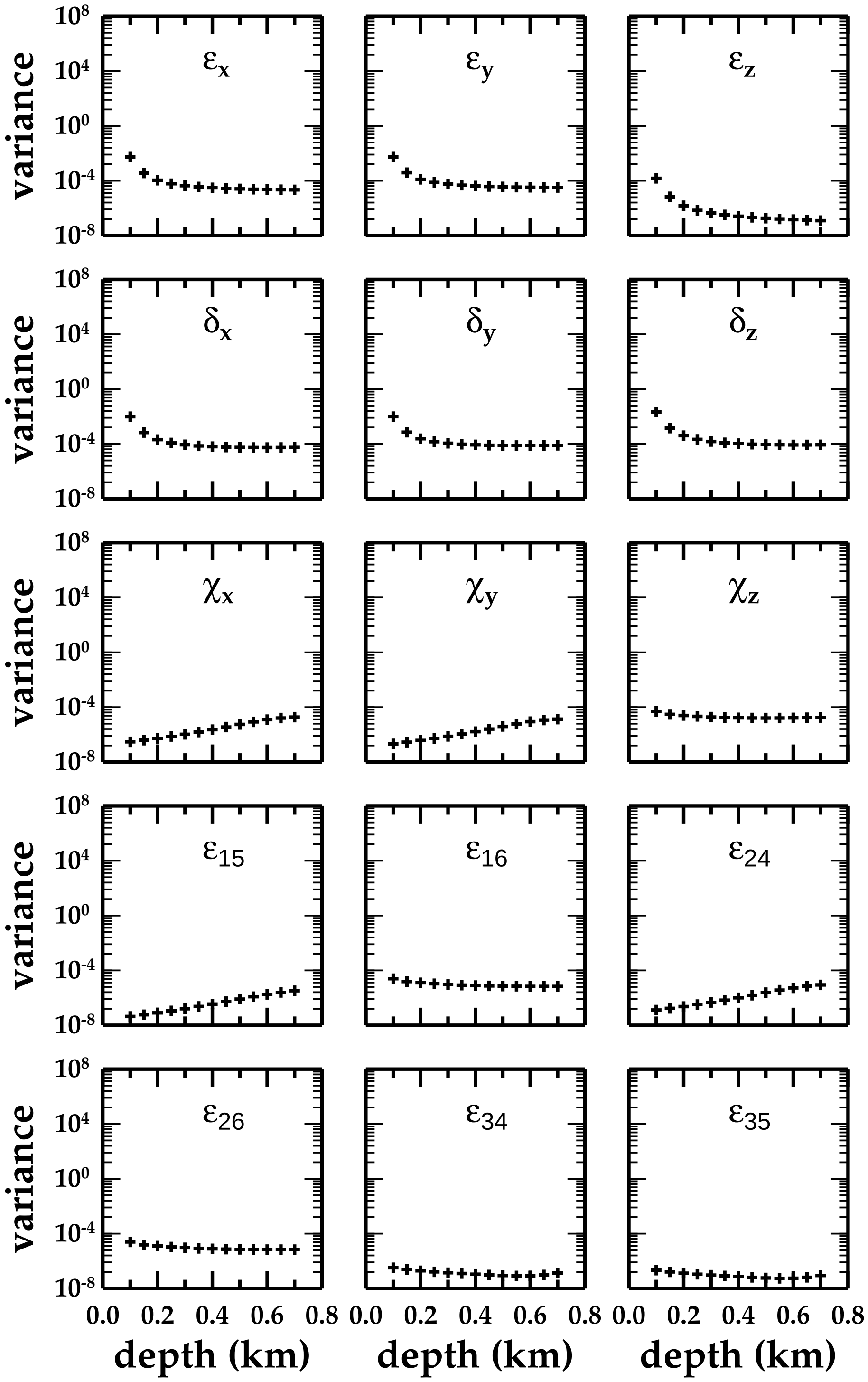
ε_x
ε_y
ε_z
δ_x
δ_y
δ_z
χ_x
χ_y
χ_z
ε_{15}
ε_{16}
ε_{24}
ε_{26}
ε_{34}
ε_{35}
variance
10^8
10^4
10^0
10^{-4}
10^{-8}
0.0
0.2
0.4
0.6
0.8
depth (km)

Figure 4b

3 PROFILES, ALL SINGULAR VALUES

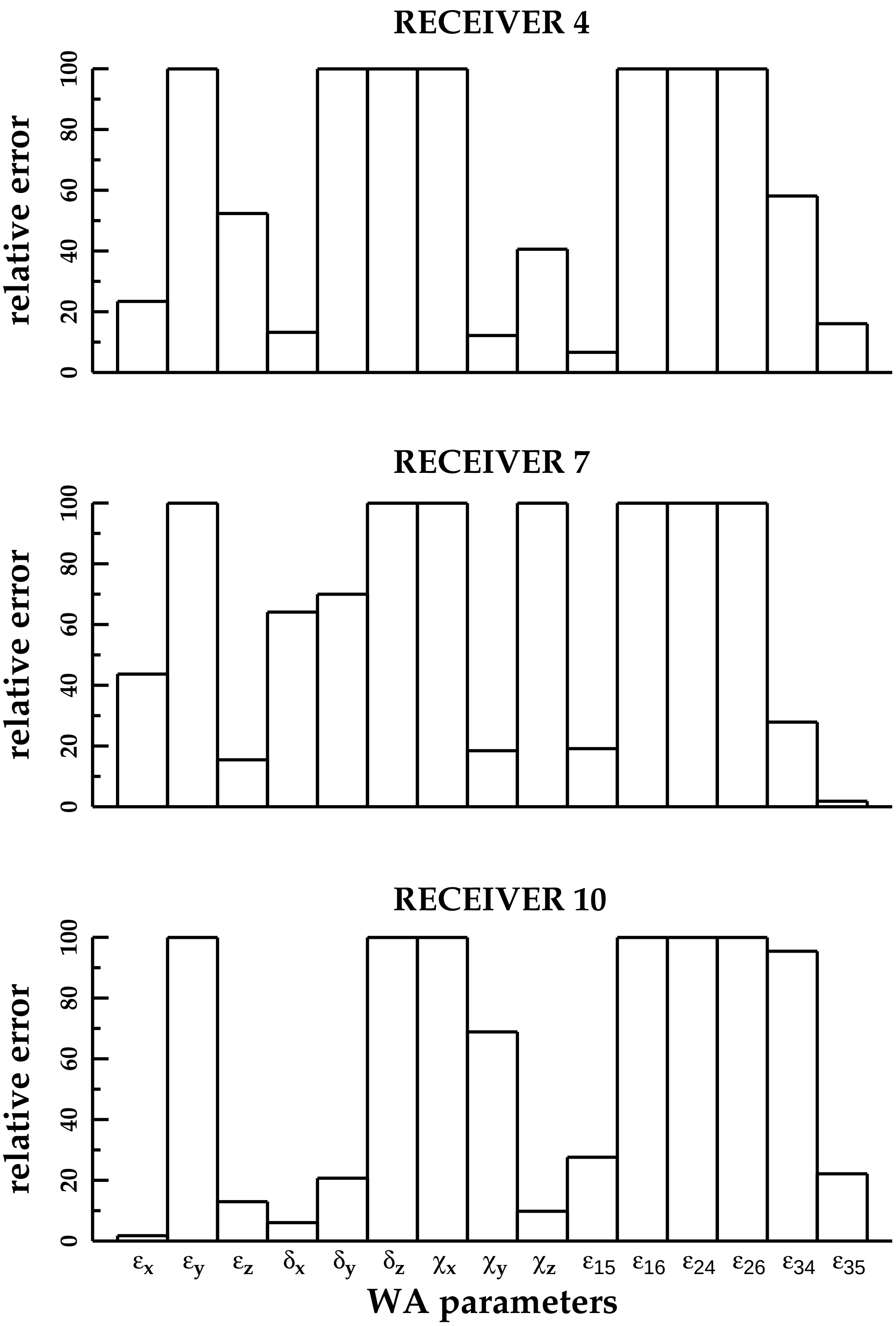

Figure 5a

3 PROFILES, 3 SINGULAR VALUES IGNORED

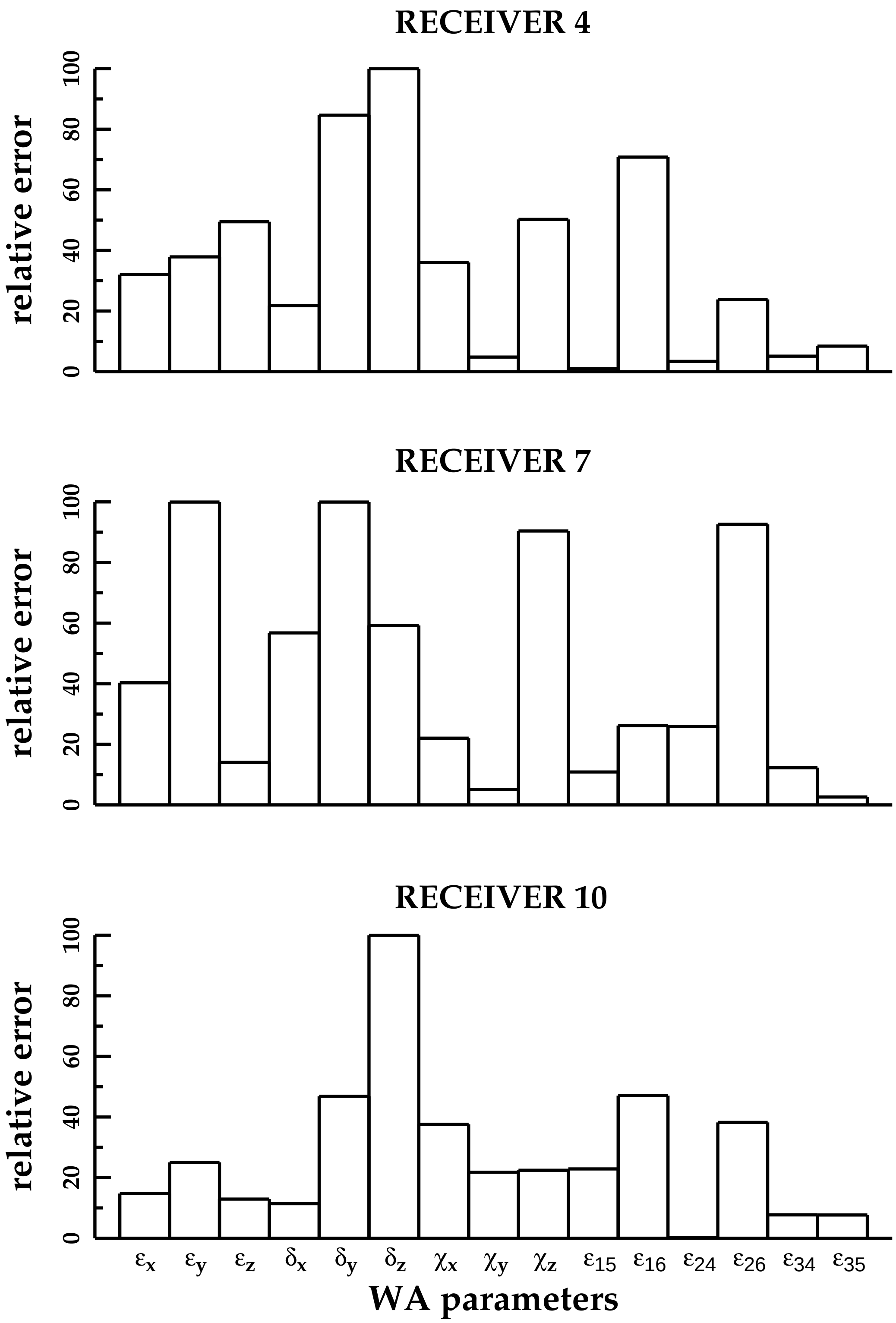

Figure 5b

5 PROFILES, ALL SINGULAR VALUES

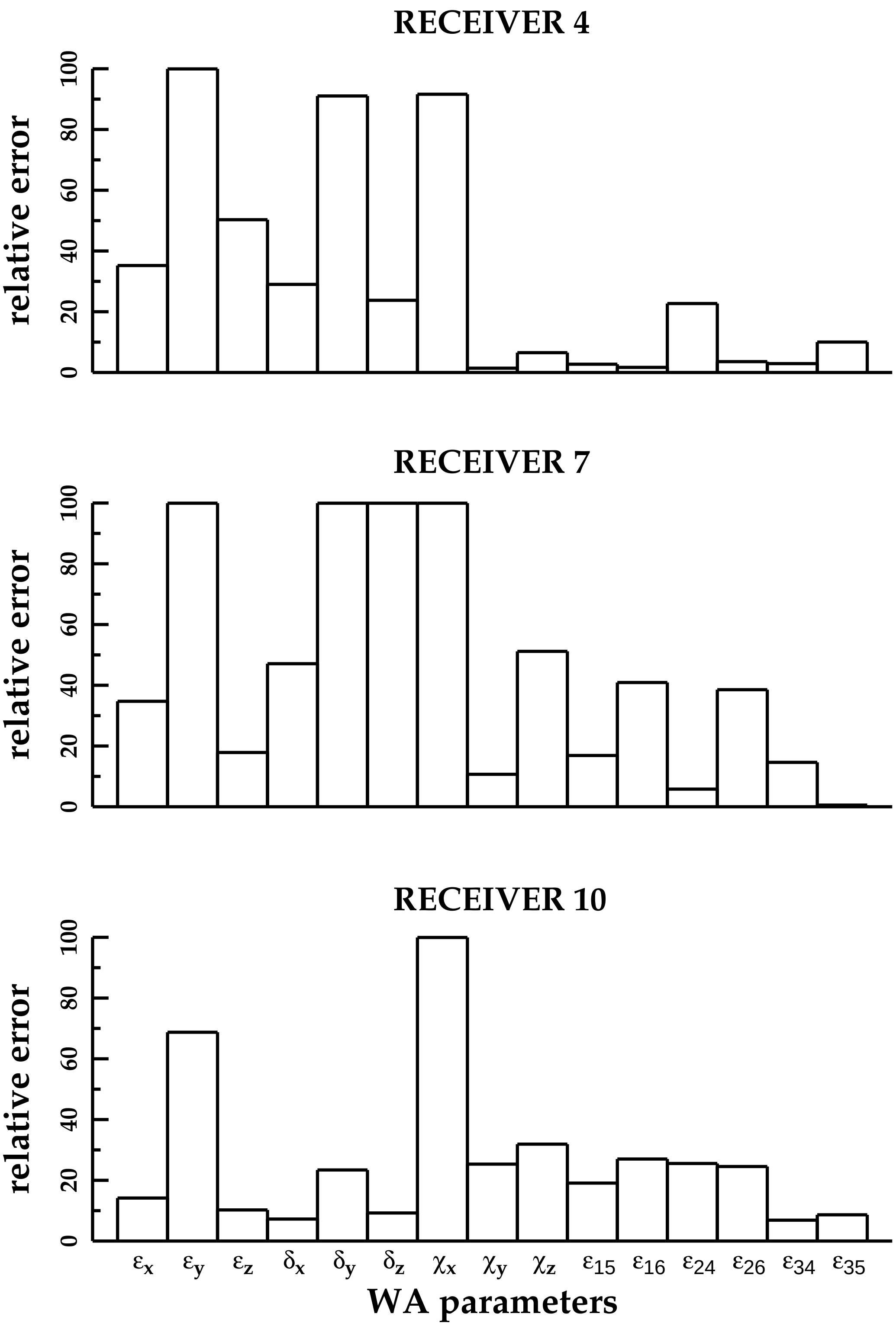

Figure 5c

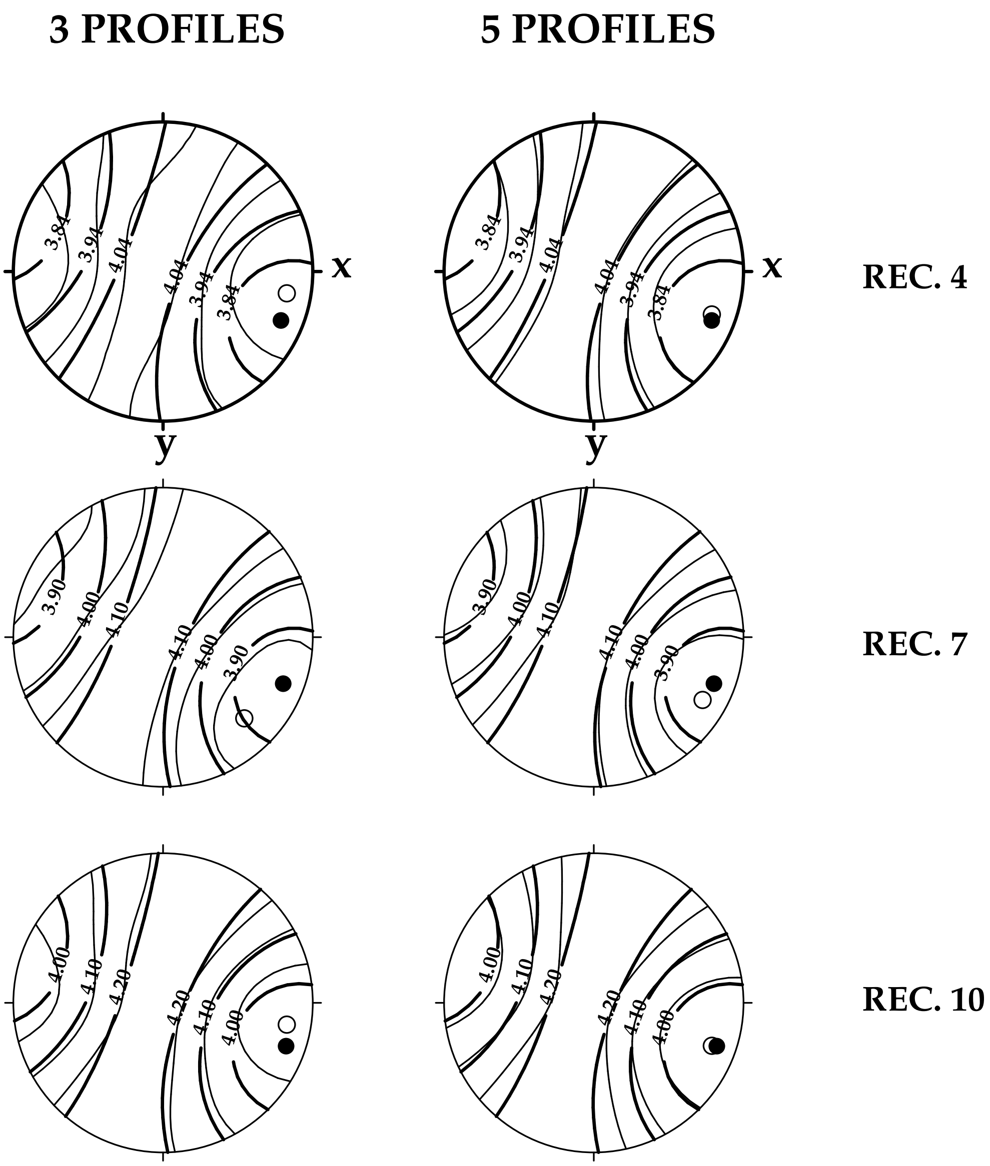
3 PROFILES
5 PROFILES
x
y
3.84
3.94
4.04
3.90
4.00
4.10
4.20
REC. 4
REC. 7
REC. 10

Figure 6

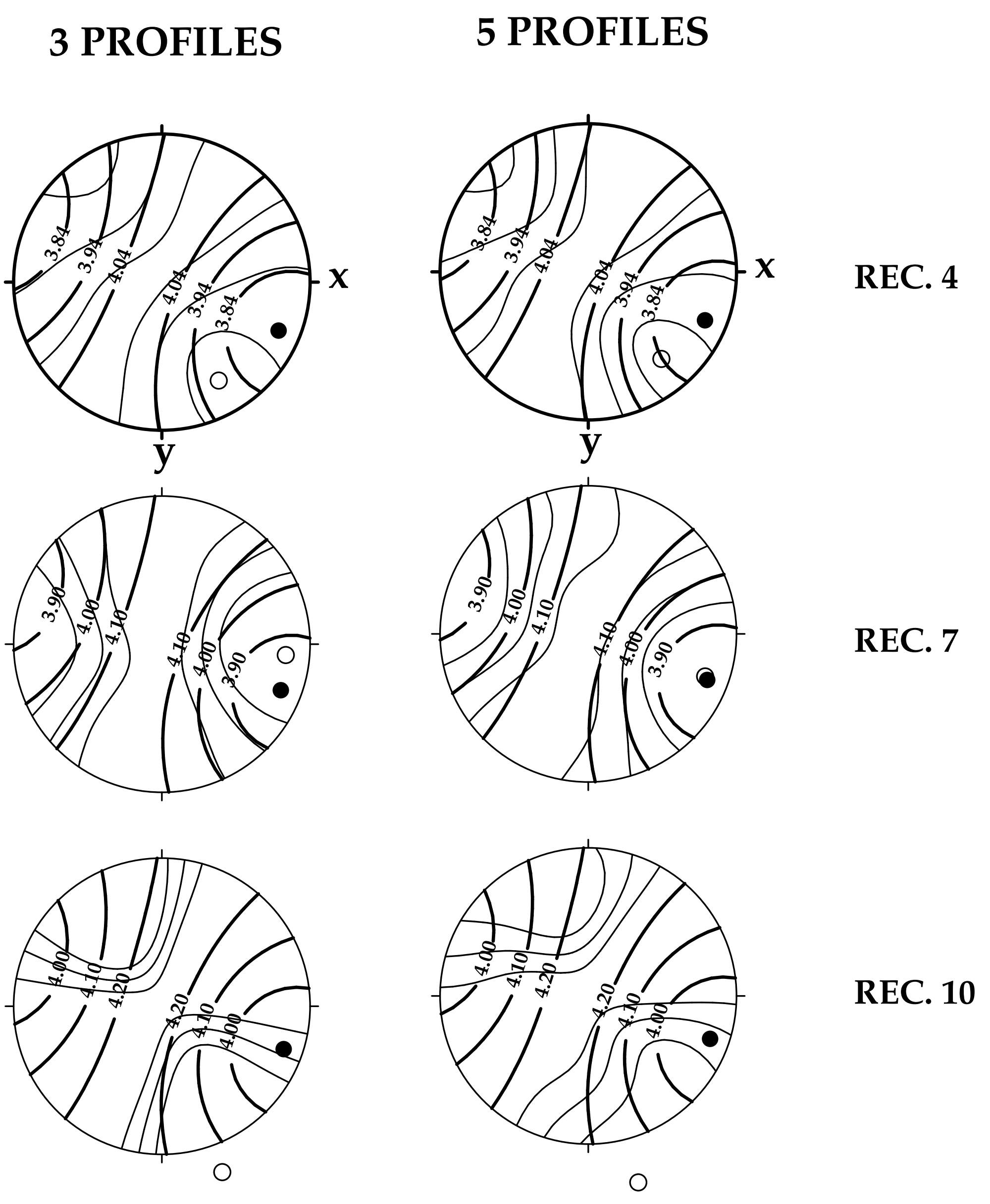
3 PROFILES
5 PROFILES
x
y
3.84
3.94
4.04
3.90
4.00
4.10
4.20
REC. 4
REC. 7
REC. 10

Figure 7